Journal of Engineering Mathematics **31:** 259–268, 1997.

On hydrodynamic instability of the flame-wedge

S.S. MINAEV[1] and G.I. SIVASHINSKY[2,3]
[1]*The Institute for Chemical Kinetics and Combustion, Russian Academy of Sciences, Siberian Branch, Novosibirski 630090, Russia.*
[2,3]*School of Mathematical Sciences, Tel Aviv University, Ramat-Aviv, Tel Aviv 69978, Israel. The Benjamin Levich Institute for Physico-Chemical Hydrodynamics, City College of the City University of New York, NY 10031, U.S.A.*

Received 24 April 1996; accepted in revised form 28 October 1996

Abstract. The hydrodynamic stability of the premixed wedge-shaped flame involving a burned-gas stagnation zone is considered. It is shown that the Darrieus-Landau instability of the flame interface is reinforced by the Kelvin-Helmholtz instability of the stagnation-zone boundary.

Key words: premixed flames, flame instability, fluid mechanics, combustion

1. Introduction

Due to burned-gas thermal expansion there is a coupling between the premixed flame and the adjacent flow-field. The most prominent manifestations of this interaction are the long-wavelength instability of a planar flame and vortex shedding induced by the flame interface [1–2]. Although in reality the two effects often coexist, the mechanism responsible for flame instability is not directly connected to vortex production. One can successfully describe the instability within a purely potential model [3–5]. On the other hand, the vortical flow behind the flame may well become unstable in its own right, thereby markedly affecting the flame dynamics. The geometrically simplest situation where one can observe this interaction is the wedge-shaped flame attached to the slot Bunsen-type burner. In such a system the streamlines crossing the flame are refracted forming the wedge-like stagnation zone with a shear, *i.e.* vortical flow near its boundary. The stability of this configuration is the main concern of the present study. The problem is analyzed within the framework of the conventional ideal-fluid-based model, where the flame is regarded as a hydrodynamic discontinuity moving at a constant normal speed and separating the fresh mixture from the combustion products. In a two-dimensional formulation, the undisturbed flame interface appears as a wedge formed by two half-planes. Figure 1 shows a general view of the undisturbed flame-flow configuration. Due to thermal expansion of the burned gas, the normal component of the flow velocity jumps up as it crosses the flame interface. The tangential component, however, remains continuous.

In the burned-gas region, owing to the streamlines refracting, we obtain the wedge-shaped interface of the localized vorticity, *i.e.* tangential discontinuity of the velocity field.

To simplify calculations, the perturbed picture is assumed to be symmetric relative to the y-axis. Far away from the flame tip, where the mutual influence of the disturbances developing on the lateral sides of the flame-wedge is negligibly weak, the disturbances grow according to the classical Darrieus-Landau solution for a freely propagating planar flame [1–2]. The only difference is that now the disturbances drift at a constant velocity towards the flame tip. Behind the flame, in the region of combustion products, the disturbances on the tangential discontinuity also drift, but now away from the tip. Far from the tip their dynamics is subjected

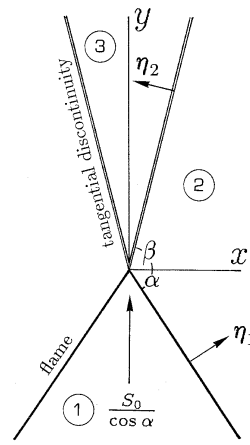

Figure 1. The undisturbed picture of the wedge-flame flow field. The numbers 1, 2, 3 denote the regions of fresh gas, combustion products and stagnation zone, respectively. The vectors $\boldsymbol{\eta}_1, \boldsymbol{\eta}_2$ are the normals to the flame interface and the tangential discontinuity.

to the Kelvin-Helmholtz instability. Near the tip the perturbations evolving on the flame and tangential discontinuity influence each other and the general picture is more involved.

2. Undisturbed flow field

Let us assume that the incoming flow of the fresh mixture moves at a constant velocity V_{1y} along the y-axis as shown on Figure 1. The normal projection of this velocity on the flame interface is equal to the flame speed, S_0, regarded as a prescribed parameter. Hence, the inclination angle of the planar flame interface, α, is determined by the simple relation

$$\cos\alpha = S_0/V_{1y}. \tag{2.1}$$

In the burned-gas region the flow field meeting the usual requirement of mass and continuity reads

$$V_{2y} = S_0 \sin\alpha(\tan\alpha + E\cot\alpha), \qquad V_{2x} = (E-1)S_0\sin\alpha. \tag{2.2–2.3}$$

Here $E = \rho_1/\rho_2$ is the thermal-expansion parameter with $E > 1$; x, y correspond to x, y-velocity components; subscripts 1, 2 correspond to the fresh and burned gas, respectively. The inclination angles of the flame, α, and tangential discontinuity, β, are related through the condition

$$(E-1)\tan\beta = (\tan\alpha + E\cot\alpha) \tag{2.4}$$

In the stagnation zone the gas is at rest and the density is identical to that of the burned gas, ρ_2. Note that

$$\beta \to \pi/2 \quad \text{as} \quad E \to 1 \tag{2.5}$$

and $\alpha - \beta \to \pi \quad$ as $E \to \infty$.

The normals and tangentials to the flame- and stagnation-zone boundary read

$$\begin{aligned} \boldsymbol{\eta}_1 &= \cos\alpha\,\mathbf{i}_y + \sin\alpha\,\mathbf{i}_x, \qquad & \boldsymbol{\zeta}_1 &= -\sin\alpha\,\mathbf{i}_y + \cos\alpha\,\mathbf{i}_x, \\ \boldsymbol{\eta}_2 &= \cos\beta\,\mathbf{i}_y - \sin\beta\,\mathbf{i}_x, \qquad & \boldsymbol{\zeta}_2 &= -\sin\beta\,\mathbf{i}_y + \cos\beta\,\mathbf{i}_x. \end{aligned} \tag{2.6}$$

Here, the subscripts 1, 2 correspond to the flame interface and tangential discontinuity, respectively. Further, $\mathbf{i}_x$ and $\mathbf{i}_y$ are the unit vectors along the x. And y-axes, respectively.

For the sequel it is convenient to introduce the new coordinates

$$\eta_1 = \boldsymbol{\eta}_1 \cdot \mathbf{X}, \qquad \eta_2 = \boldsymbol{\eta}_2 \cdot \mathbf{X}; \qquad \zeta_1 = \boldsymbol{\zeta}_1 \cdot \mathbf{X}, \qquad \zeta_2 = \boldsymbol{\zeta}_2 \cdot \mathbf{X}, \tag{2.7}$$

where $X = (x, y)$.

In these variables the undisturbed interfaces for the flame and tangential discontinuity become $\eta_1 = 0$ and $\eta_2 = 0$, respectively. Note that the directions of the normals $\boldsymbol{\eta}_1$ and $\boldsymbol{\eta}_2$ at the interfaces coincide with those of the azimuthal derivatives in polar coordinates.

3. Equations and boundary conditions

The hydrodynamic disturbances in all regions are described by the linearized Euler equations. In the fresh-gas region the equations written in the coordinates η_1 and ζ_1 read

$$\frac{\partial v_1}{\partial t} + S_0 \frac{\partial v_1}{\partial \eta_1} - S_0 \tan\alpha \frac{\partial v_1}{\partial \zeta_1} = -\frac{1}{\rho_1}\frac{\partial p_1}{\partial \eta_1}, \tag{3.1}$$

$$\frac{\partial u_1}{\partial t} + S_0 \frac{\partial u_1}{\partial \eta_1} - S_0 \tan\alpha \frac{\partial u_1}{\partial \zeta_1} = -\frac{1}{\rho_1}\frac{\partial p_1}{\partial \zeta_1}, \tag{3.2}$$

$$\frac{\partial u_1}{\partial \zeta_1} + \frac{\partial v_1}{\partial \eta_1} = 0. \tag{3.3}$$

Here, v_1, u_1 are the velocity component along $\boldsymbol{\eta}_1, \boldsymbol{\zeta}_1$; p_1, ρ_1 are the fresh-mixture pressure and density. In the burned-gas region, it is helpful to have the hydrodynamic equations written both in (η_1, ζ_1) and (η_2, ζ_2) coordinates. In the coordinates (η_1, ζ_1) the system reads

$$\frac{\partial v_{21}}{\partial t} + ES_0 \frac{\partial v_{21}}{\partial \eta_1} - S_0 \tan\alpha \frac{\partial v_{21}}{\partial \zeta_1} = -\frac{E}{\rho_1}\frac{\partial p_2}{\partial \eta_1}, \tag{3.4}$$

$$\frac{\partial u_{21}}{\partial t} + ES_0 \frac{\partial u_{21}}{\partial \eta_1} - S_0 \tan\alpha \frac{\partial u_{21}}{\partial \zeta_1} = -\frac{E}{\rho_1}\frac{\partial p_2}{\partial \zeta_1}, \tag{3.5}$$

$$\frac{\partial u_{21}}{\partial \zeta_1} + \frac{\partial v_{21}}{\partial \eta_1} = 0. \tag{3.6}$$

In the coordinates (η_2, ζ_2) we obtain

$$\frac{\partial v_{23}}{\partial t} + U_0 \frac{\partial v_{23}}{\partial \zeta_2} = -\frac{E}{\rho_1}\frac{\partial p_2}{\partial \eta_2}, \tag{3.7}$$

$$\frac{\partial u_{23}}{\partial t} + U_0 \frac{\partial u_{23}}{\partial \zeta_2} = -\frac{E}{\rho_1}\frac{\partial p_2}{\partial \zeta_2}, \tag{3.8}$$

$$\frac{\partial u_{23}}{\partial \zeta_2} + \frac{\partial v_{23}}{\partial \eta_2} = 0. \tag{3.9}$$

Here, v_{21}, u_{21} are the flow-velocity components along $\boldsymbol{\eta}_1$ and $\boldsymbol{\zeta}_1$ and v_{23}, u_{23} – along $\boldsymbol{\eta}_2$ and $\boldsymbol{\zeta}_2$ and p_2 is the pressure; $U_0 = (E-1)S_0 \sin\alpha/\cos\beta$ is the unperturbed velocity of the burned gas along the stagnation-zone boundary.

In the stagnation zone the hydrodynamic equations written in the coordinates (η_2, ζ_2) read

$$\frac{\partial v_3}{\partial t} = -\frac{E}{\rho_1}\frac{\partial p_3}{\partial \eta_2}, \qquad \frac{\partial u_3}{\partial t} = -\frac{E}{\rho_1}\frac{\partial p_3}{\partial \zeta_2}, \qquad \frac{\partial u_3}{\partial \zeta_2} + \frac{\partial v_3}{\partial \eta_2} = 0. \tag{3.10–3.12}$$

Here, v_3, u_3 are the velocity components along $\boldsymbol{\eta}_2$ and $\boldsymbol{\zeta}_2$ and p_3 is the pressure. It is assumed that the gas density in the stagnation zone is identical to that of the burned gas, *viz.* $\rho_2 = \rho_1/E$. Let us now turn to the conditions at the interfaces and denote the profiles of the disturbed flame and the tangential discontinuity as $\eta_1 = f_1(\zeta_1, t)$ and $\eta_2 = f_2(\zeta_2, t)$, respectively.

For the undisturbed interfaces we have $\eta_1 = \eta_2 = 0$. The interfacial disturbances of velocity and pressure depend only on the distance from the flame tip and on time. It is, therefore, convenient to introduce the polar coordinates (r, φ) with the origin at the flame tip. At the interfaces: $\partial/\partial\xi_1 = \partial/\partial\xi_2 = \partial/\partial r$.

The boundary conditions at the flame interface read

$$\widehat{L}_1 f_1 = v_1, \qquad \widehat{L}_2 f_1 = v_{21}, \tag{3.13–3.14}$$

$$u_1 - u_{21} = (E-1)S_0 \partial f_1/\partial r, \qquad p_1 = p_2 = a_1, \tag{3.15–3.16}$$

where $\widehat{L}_1 = \partial/\partial t - S_0 \tan\alpha \partial/\partial r$. The conditions (3.13) (3.14) express conservation of mass and the flame-speed constancy. The momentum flux conservation is described by (3.15–3.16).

The boundary conditions on the tangential discontinuity read

$$\widehat{L}_2 f_2 = v_{23}, \qquad \partial f_2/\partial t = v_3, \qquad p_2 = p_3 = a_2, \tag{3.17–3.19}$$

where $\widehat{L}_2 = \partial/\partial t + U_0 \partial/\partial r$.

4. Equations for the disturbed interfaces

In this section, the stability problem is reduced to a set of coupled equations for the disturbed interfaces η_1 and η_2. First, as is readily seen, the perturbation of pressure in all three regions is described by the Laplace equation subject to the boundary conditions (3.16), (3.19). It is required that the perturbation of pressure as well as its radial derivatives coincide at $r = 0$. It is also required that the radial derivatives of all the quantities involved vanish as $r \to \infty$. Hence, p_1, p_2, p_3 may be written as a convolution of a_1 and a_2 with the associated Green functions

$$p_1 = \widehat{G}_1 a_1, \qquad p_2 = \widehat{G}_{21} a_1 + \widehat{G}_{23} a_2, \qquad p_3 = \widehat{G}_3 a_2. \tag{4.1}$$

The operators $\widehat{G}_1, \widehat{G}_{21}, \widehat{G}_{23}$ and $\widehat{G}_3$ correspond to the fresh and burned gases and stagnation region, respectively. Their concrete structure is given in the Appendix.

Let us assume that in the fresh gas and stagnation regions the flow is potential. Thus, if we know the fresh-gas normal velocity along the flame interface we may calculate its value at any

point in the fresh-gas region. The same is true for the stagnation zone as well. The boundary conditions (3.13) and (3.18), therefore, yield

$$v_1 = \widehat{G}_1 \widehat{L}_1 f_1, \qquad v_3 = \widehat{G}_3 \partial f_2 / \partial t. \tag{4.2}$$

Hence

$$\left.\frac{\partial v_1}{\partial \eta_1}\right|_{\eta_1=0} = \widehat{K}_1 \widehat{L}_1 f_1, \qquad \left.\frac{\partial v_3}{\partial \eta_2}\right|_{\eta_2=0} = \widehat{K}_3 \frac{\partial f_2}{\partial t}, \tag{4.3}$$

where the operators $\widehat{K}_1$ and $\widehat{K}_3$ are defined as

$$\widehat{K}_1 = \lim_{\eta_1 \to 0} \frac{\partial}{\partial \eta_1} \widehat{G}_1, \qquad \widehat{K}_3 = \lim_{\eta_2 \to 0} \frac{\partial}{\partial \eta_2} \widehat{G}_3. \tag{4.4}$$

For their detailed structure see the Appendix. We also introduce the new operators $\widehat{K}_{21}, \widehat{K}_{23}$, defined as

$$\widehat{K}_{21} = \lim_{\eta_1 \to 0} \frac{\partial}{\partial \eta_1} \widehat{G}_{21} = \lim_{\varphi \to -\alpha} \frac{1}{r} \frac{\partial}{\partial \varphi} \widehat{G}_{21} = -\lim_{\varphi \to \beta} \frac{1}{r} \frac{\partial}{\partial \varphi} \widehat{G}_{23}, \tag{4.5}$$

$$\widehat{K}_{23} = \lim_{\eta_1 \to 0} \frac{\partial}{\partial \eta_1} \widehat{G}_{23} = \lim_{\varphi \to -\alpha} \frac{1}{r} \frac{\partial}{\partial \varphi} \widehat{G}_{23} = -\lim_{\varphi \to \beta} \frac{1}{r} \frac{\partial}{\partial \varphi} \widehat{G}_{21}. \tag{4.6}$$

The approach leading to the equations for the interfaces may be described as follows. Equations (3.1) and (3.4) on the flame interface read

$$\widehat{L}_1^2 f_1 + S_0 \widehat{K}_1 v_1 = -\frac{1}{\rho_1} \widehat{K}_1 a_1, \tag{4.7}$$

$$\frac{1}{E} \widehat{L}_1^2 f_1 + S_0 \left.\frac{\partial v_{21}}{\partial \eta_1}\right|_{\eta_1=0} = -\frac{1}{\rho_1} (\widehat{K}_{21} a_1 + \widehat{K}_{23} a_2). \tag{4.8}$$

Here we used the expressions (4.3) and (3.19). Employing the continuity equations (3.3) and (3.6), we may write the relations (4.7) (4.8) as follows:

$$\widehat{L}_1^2 f_1 - S_0 \frac{\partial u_1}{\partial r} = -\frac{1}{\rho_1} \widehat{K}_1 a_1, \tag{4.9}$$

$$\frac{1}{E} \widehat{L}_1^2 f_1 - S_0 \frac{\partial u_{21}}{\partial r} = -\frac{1}{\rho_1} (\widehat{K}_{21} a_1 + \widehat{K}_{23} a_2). \tag{4.10}$$

Subtracting (4.9) from (4.10) and employing the boundary condition (3.15), we obtain

$$\left(\frac{1}{E} - 1\right) \widehat{L}_1^2 f_1 + (E-1) S_0^2 \frac{\partial^2 f_1}{\partial r^2} = \frac{1}{\rho_1} ((\widehat{K}_1 - \widehat{K}_{21}) a_1 - \widehat{K}_{23} a_2). \tag{4.11}$$

Equations (3.7) and (3.10) on the tangential discontinuity interface may be written as

$$\widehat{L}_2 v_{23} = \widehat{L}_2^2 f_2 = \frac{E}{\rho_1} (\widehat{K}_{21} a_2 + \widehat{K}_{23} a_1), \tag{4.12}$$

$$\frac{\partial^2 f_2}{\partial t^2} = -\frac{E}{\rho_1}\widehat{K}_3 a_2. \tag{4.13}$$

The Equations (4.10), (4.11), (4.12) and (4.13), which account for the boundary condition (3.13), constitute the system that describes evolution of the interfaces f_1, f_2 as well as the interfacial pressures a_1 and a_2.

$$\widehat{L}_1^2 f_1 + S_0 \widehat{K}_1 \widehat{L}_1 f_1 = -\frac{1}{\rho_1}\widehat{K}_1 a_1, \tag{4.14}$$

$$\left(\frac{1}{E} - 1\right)\widehat{L}_1^2 f_1 + (E-1)S_0^2 \frac{\partial^2 f_1}{\partial r^2} = \frac{1}{\rho_1}((\widehat{K}_1 - \widehat{K}_{21})a_1 - \widehat{K}_{23}a_2) \tag{4.15}$$

$$\frac{\partial^2 f_2}{\partial t^2} = -\frac{E}{\rho_1}\widehat{K}_3 a_2, \qquad \widehat{L}_2^2 f_2 = \frac{E}{\rho_1}(\widehat{K}_{21}a_2 + \widehat{K}_{23}a_1). \tag{4.16–4.17}$$

Eliminating a_1 and a_2, we end up with the system just for the interfaces η_1, η_2.

5. Correspondence with the Darrieus-Landau and Kelvin-Helmholtz solutions

The transition to the Darrieus-Landau problem is realized at $r \to \infty$. In this limit the equations (4.14) (4.15) become

$$\widehat{L}_1^2 f_1 + S_0 \widehat{L}_1 \widehat{K} f_1 = -\frac{1}{\rho_1}\widehat{K} a_1, \tag{5.1}$$

$$\left(\frac{1}{E} - 1\right)\widehat{L}_1^2 f_1 + (E-1)S_0^2 \frac{\partial^2 f_1}{\partial r^2} = \frac{2}{\rho_1}\widehat{K} a_1, \tag{5.2}$$

where $\widehat{K}$ is the Hilbert operator (see A.7). Eliminating a_1 and setting $f_2 = \exp(\Omega t + ikr)$ we end up with a relation between Ω and k. The only deviation from the Darrieus-Landau solution in that the instability rate, Ω, acquires the imaginary part, $\mathrm{Im}\,\Omega = S_0 k \tan\alpha$. The Darrieus-Landau dispersion relation naturally arises at $\alpha = 0$.

For the disturbed tangential discontinuity the pertinent equations at $r \to \infty$ are identical to those for a plane interface separating two gases of equal densities, but different velocities along the boundary.

In the stagnation zone the gas is at rest, while the burned gas moves at the velocity $U_0 = (E-1)S_0 \sin\alpha/\cos\beta$ along the border. Hence, the pertinent dispersion relation reads

$$\Omega = \tfrac{1}{2}U_0(-ik \pm |k|), \tag{5.3}$$

recovering the classical Kelvin-Helmholtz solution (*e.g.* [6, pp. 481–486])

6. Narrow-wedge approximations

In this section we consider two limiting situations where the fresh gas or the stagnation regions form sharp wedges. The problems are considered independently and we ignore interaction between the interfaces. Apart from this, the interfacial dynamics is considered far from the

wedge tip. The flame disturbances are described by (4.14) and (4.15). For weak thermal expansion $E-1=\varepsilon\ll 1$ the latter become

$$\hat{L}_1^2 f_1 + S_0\widehat{K}_1\hat{L}_1 f_1 = -\frac{1}{\rho_1}\widehat{K}_1 a_1, \tag{6.1}$$

$$-\varepsilon\hat{L}_1^2 f_1 + \varepsilon S_0^2\frac{\partial^2 f_1}{\partial r^2} = \frac{1}{\rho_1}(\widehat{K}_1 - \widehat{K})a_1, \tag{6.2}$$

In the narrow-wedge limit $\pi/2-\alpha=\gamma\ll 1$ the operators $\widehat{K}_1$ and $\hat{L}_1$ are simplified to

$$\widehat{K}_1 = -\gamma\frac{\partial}{\partial r}\left(r\frac{\partial}{\partial r}\right), \qquad \hat{L}_1 = \frac{\partial}{\partial t} - \frac{1}{\gamma}S_0\frac{\partial}{\partial r}. \tag{6.3–6.4}$$

The relation (6.3) is obtained from the following arguments. Within the wedge we have

$$\frac{\partial}{\partial r}\left(r\frac{\partial p}{\partial r}\right) + \frac{1}{r}\frac{\partial^2 p}{\partial\varphi^2} = 0,$$

while at the boundary $p_1=a_1$. For disturbances that are symmetrical relative to the y-axis we have

$$\frac{\partial^2 p_1}{\partial\varphi^2} \simeq \frac{1}{\gamma}\frac{\partial p_1}{\partial\varphi}\bigg|_{\varphi=-\alpha} = \frac{1}{\gamma}r\widehat{K}_1 a_1. \tag{6.5}$$

The system (6.1) (6.2), thus, is reduced to a single equation for f_1,

$$(\hat{L}_1^2 + S_0\widehat{K}_1 L_1 - \varepsilon S_0^2\widehat{K}_1\widehat{K})f_1 = 0. \tag{6.6}$$

Substituting $f_1=\exp(\Omega t+ikr)$ and replacing, for simplicity, $\widehat{K}_1$ by $-\gamma\partial/\partial r$, we obtain

$$\Omega = S_0 K\left(i/j + \gamma\frac{kr}{2}(\sqrt{1+4\varepsilon/\gamma kr}-1)\right). \tag{6.7}$$

For the sharp wedge, therefore, the disturbances grow much slower than for a plane flame where, as is well-known [6],

$$\Omega = \tfrac{1}{2}\varepsilon S_0|k|. \tag{6.8}$$

Note that for a more accurate analysis of Equation (6.6) the *ansatz* $f_1=\exp(\Omega t+ikr)$ should be modified in accordance with the actual structure (6.3) of $\widehat{K}_1$.

Now consider stability of the tangential discontinuity at $\gamma=\pi/2-\beta\ll 1$. In this case the interface evolution is described by (4.16) and (4.17), where a_1 should be set to zero and $\widehat{K}_{21}$ replaced by the Hilbert operator, $\widehat{K}$, *i.e.*

$$\frac{\partial^2 f_2}{\partial t^2} = -\frac{E}{\rho_1}\widehat{K}_3 a_2, \qquad -\hat{L}_2^2 f_2 = \frac{E}{\rho_1}\widehat{K}a_2. \tag{6.9–6.10}$$

Adopting the same approach as for the sharp flame wedge, we may approximate $\widehat{K_3}$ by $\nu r\partial^2/\partial r^2$, where $\nu = \pi/2 - \beta \ll 1$. The resulting dispersion relation reads

$$\Omega = kU_0\sqrt{\nu rk}(\pm 1 - i\sqrt{\nu rk})/(1+\nu rk). \tag{6.11}$$

Thus, for symmetric disturbances the growth rate appears to be lower than for a planar interface; see (5.3). The analysis presented in this section is valid only in the domain $0 < kr < 1/\gamma$. For larger r, for which the mutual influence of the lateral surfaces of the wedge may be neglected, the growth rate of the disturbances will be described by the Darrieus-Landau and Kelvin-Helmholtz solutions.

7. Flame interface and stagnation-zone-boundary interaction

We will study the stability problem, assuming the thermal expansion to be weak ($E - 1 = \varepsilon \ll 1$), and the fresh-gas wedge to the blunt ($\alpha \ll 1$).

The system (4.14–4.17) becomes

$$S_0\frac{\partial f_1}{\partial t} = -\frac{a_1}{\rho_1}, \tag{7.1}$$

$$\varepsilon S_0^2\frac{\partial^2 f_1}{\partial r^2} = \frac{1}{\rho_1}(\widehat{K}_1 - \widehat{K}_{21})a_1 - \frac{1}{\rho_1}\widehat{K}_{23}a_2, \tag{7.2}$$

$$\frac{\partial^2 f_2}{\partial t^2} = -\frac{1}{\partial_1}\widehat{K}_3 a_2, \quad \widehat{L}_2^2 f_2 = \frac{1}{\partial_1}(\widehat{K}_{21}a_2 + \widehat{K}_{23}a_1). \tag{7.3–7.4}$$

Eliminating f_1 and f_2, we obtain two coupled equations for the interfacial pressures a_1 and a_2:

$$-\varepsilon S_0\frac{\partial^2 a_1}{\partial r^2} = (\widehat{K}_1 - \widehat{K}_{21})\frac{\partial a_1}{\partial t} - \widehat{K}_{23}\frac{\partial a_2}{\partial t}, \tag{7.5}$$

$$-\widehat{L}_2^2\widehat{K}_3 a_2 = \widehat{K}_{21}\frac{\partial^2 a_r}{\partial t^2} + \widehat{K}_{23}\frac{\partial^2 a_1}{\partial t^2}. \tag{7.6}$$

Since at $\alpha \ll 1$ the stagnation zone wedge is sharp ($\pi/2 - \beta = \gamma \ll 1$), the system (7.5)–(7.6) allows for further simplification:

$$\varepsilon S_0\frac{\partial^2 a_1}{\partial r^2} = -2\widehat{K}\frac{\partial a_1}{\partial t} + \widehat{K}_{23}\frac{\partial a_2}{\partial t}, \quad \nu r S_0^2\frac{\partial^3 a_2}{\partial r^3} = \widehat{K}\frac{\partial^2 a_2}{\partial t^2} - K_{23}\frac{\partial^2 a_1}{\partial t^2}. \tag{7.7–7.8}$$

Here $\widehat{K_3}$ is replaced by $\nu r\partial/\partial r$. Near the tip, where interaction between the interfaces is anticipated to be most prominent, the operator $\widehat{K_{23}}$. At the system (7.7)–(7.8) describes the dynamics of a planar flame. Since ν is small, its impact may be evaluated iteractively.

Thus, as we would expect, the flame instability is markedly reinforced by the presence of the tangential discontinuity – the instability of the downstream vortical flow. The latter is likely to result in an additional extension of the wrinkled flame interface and, thereby, in burning-rate enhancement.

In the wedge flames discussed in this paper the basic vortical flow is controlled by the incoming flow velocity V_{1y}. A similar effect, however, may occur in freely propagating flames subjected to a Darrieus-Landau instability as well. Here, the vortical flow sustained by the flame cusp may undergo self-turbulization and, as in the previous problem, promote flame wrinkling and, thus, elevate its propagation speed.

Appendix

As is well-known, solution of the Dirichlet problem for the upper half-plane may be written as

$$\Phi(\xi,\tau) = \frac{1}{\pi}\int_{-\infty}^{\infty} \frac{\tau\varphi(\nu)}{\tau^2+(\xi-\nu)^2}\,\mathrm{d}\nu. \tag{A.1}$$

Here $\Phi(\xi,\tau)$ is a harmonic function at $\tau > 0$ and $\varphi(\xi) = \Phi(\xi,0)$. To solve the Dirichlet problem for the fresh-gas sector $\pi-\alpha < \theta < 2\pi-\alpha$, we may use the conformal mapping

$$w = \xi + i\tau = r^{\kappa_1}\exp(i\kappa_1(\theta-\pi-\alpha)) \tag{A.2}$$

of the half-plane $\operatorname{Im} w > 0$ onto $\pi-\alpha < \theta < 2\pi-\alpha$. Here $\kappa_1 = \pi/(\pi-2\alpha)$. Under such a mapping the half-plane points go over to those of the above sector according to the transformation

$$\xi = r^{\kappa_1}\cos(\kappa_1(\theta-\pi-\alpha)), \qquad \tau = r^{\kappa_1}\sin(\kappa_1(\theta-\pi-\alpha)). \tag{A.2}$$

The ray $[0,\xi=\infty]$ corresponds to the ray $[0,(\theta=\pi+\alpha)r=\infty]$, and the ray $[0,\xi=-\infty]$ corresponds to the ray $[0,(\theta=2\pi-\alpha)\ r=\infty]$. Employing (A.2) and polar coordinates (r,θ), we may transform the integral (A.1) as follows:

$$\Phi(r,\theta) = \frac{\kappa_1}{\pi}\int_0^{\infty}\left[\frac{\tau\varphi^-(\eta)\eta^{\kappa_1-1}}{\tau^2+(\xi-\eta^{\kappa_1})^2} + \frac{\tau\varphi^+(\eta)\eta^{\kappa_1-1}}{\tau^2+(\xi+\eta^{\kappa_1})^2}\right]\mathrm{d}\eta. \tag{A.3}$$

yielding Dirichlet's solution for the sector. Here $\varphi^-(r) = \Phi(r,\pi+\alpha)$ and $\varphi^+(r) = \Phi(r,2\pi-\alpha)$. The relation (A.3) defines the operator $\widehat{G}_1$. Hence, at $\theta = 2\pi-\alpha$ we have

$$\begin{aligned}\frac{\mathrm{d}\Phi}{\mathrm{d}\eta_1} &= \frac{1}{r}\frac{\partial\Phi}{\partial\theta}\bigg|_{2\pi-\alpha} = \\ &= -\frac{\kappa_1^2 r^{\kappa_1-1}}{\pi}\int_0^{\infty}\left[\frac{\varphi^-(\eta)\eta^{\kappa_1-1}}{(r^{\kappa_1}+\eta^{\kappa_1})^2} + \frac{\varphi^+(\eta)\eta^{\kappa_1-1}}{(r^{\kappa_1}-\eta^{\kappa_1})^2}\right]\mathrm{d}\eta\end{aligned} \tag{A.4}$$

or in a form that is more convenient for further calculations:

$$\frac{1}{r}\frac{\partial\Phi}{\partial\theta}\bigg|_{2\pi-\alpha} = -\frac{\kappa_1 r^{\kappa_1-1}}{\pi}\int_0^{\infty}\left(\frac{\varphi_\eta^-}{\eta^{\kappa_1}+r^{\kappa_1}} + \frac{\varphi_\eta^+}{\eta^{\kappa_1}-r^{\kappa_1}}\right)\mathrm{d}\eta. \tag{A.5}$$

Let us define the new operator $\widehat{K}_1$ as

$$\widehat{K}_1 f(r) = -\frac{2\kappa_1 r^{\kappa_1-1}}{\pi}\int_0^{\infty}\frac{\eta^{\kappa_1} f_\eta}{\eta^{2\kappa_1}-r^{2\kappa_1}}\,\mathrm{d}\eta, \tag{A.6}$$

where the integral is understood in the principal-value sense. At $\kappa_1 = 1$ (plane flame) $\widehat{K_1}$ becomes the Hilbert operator $\widehat{K}$ for symmetric $f(r)$, *i.e.* $f(r) = f(-r)$,

$$\widehat{K}f(r) = \frac{1}{\pi}\int_{-\infty}^{\infty} \frac{f_\eta}{r-\eta}\,\mathrm{d}\eta. \tag{A.7}$$

In the general case, we should use the relation (A.5). In the limit $\kappa \to 0$, which corresponds to an infinitely sharp wedge, $\widehat{K_1}$ vanishes.

In a similar manner we may construct Green's operators for other regions of the problem. Thus, for the stagnation zone

$$\widehat{K_3}f(r) = \frac{2\kappa_3 r^{\kappa_3-1}}{\pi}\int_0^{\infty} \frac{\eta^{\kappa_3} f_\eta}{\eta^{2\kappa_3} - r^{2\kappa_3}}\,\mathrm{d}\eta, \tag{A.8}$$

where $\beta < \theta < \pi - \beta$ and $\kappa_3 = \pi/\pi - 2\beta$. For the burned gas region

$$\widehat{K_{21}}f = \frac{\kappa_2 r^{\kappa_2-1}}{\pi}\int_0^{\infty} \frac{f_\eta}{\eta^{\kappa_2} - r^{\kappa_2}}\,\mathrm{d}\eta, \tag{A.9}$$

$$\widehat{K_{23}}f = \frac{\kappa_2 r^{\kappa_2-1}}{\pi}\int_0^{\infty} \frac{f_\eta}{\eta^{\kappa_2} + r^{\kappa_2}}\,\mathrm{d}\eta, \tag{A.10}$$

where $-\alpha < \theta < \beta, \kappa_2 = \pi/\alpha + \beta$. At $r \to \infty$:

$$\widehat{K_{23}} \to 0, \qquad \widehat{K_{23}} \to \widehat{K}, \qquad \widehat{K_3} \to \widehat{K}, \qquad \widehat{K_1} \to \widehat{K}, \tag{A.11}$$

$$\widehat{K_3} \to 0 \quad \text{at } \kappa_3 \to 0 \ \text{(infinitely narrow stagnation zone)}. \tag{A.12}$$

Acknowledgements

This study was supported by the U.S. Department of Energy (Grant No. DE-FG02-88ER13822), the National Science Foundation (Grant No. CTS-9521084), the U.S.-Israel Bi-national Science Foundation (Grant No. 93-00030), the Israel Science Foundation (Grant No. 15-95-1) and the Gordon Foundation for Energy Research.

References

1. G. Darrieus, Propagation d'un front de flamme. Essai de théorie de vitesses anomales de déflagration par developpement spontané de la turbulence. Unpublished typescript of paper given at the *Sixth International Congress of Applied Mechanics*, Paris 1946; mentioned in G. Darrieus. La mécanique des fluides – quelques progrès récents. *La Technique Moderne Supplément* 31(15) (1938) pp. 9–17.
2. L. D. Landau, On the theory of slow combustion. *Acta Physicochim. URSS.* 19 (1944) 77–85.
3. G. I. Sivashinsky, Nonlinear analysis of hydrodynamic instability in laminar flames, Part I. Derivation of basic equations. *Acta Astronautica* 4 (1977) 1177–1206.
4. G. I. Sivashinsky and P. Clavin, On the nonlinear theory of hydrodynamic instability in flames. *J. Physique.* 48 (1987) 193–198.
5. M. L. Frankel, An equation of surface dynamics modeling flame fronts as density discontinuities in potential flows. *Physics of Fluids* A2 (1990) 1879–1883.
6. S. Chandrasekhar, *Hydrodynamic and Hydromagnetic Stability.* Oxford: Oxford University Press (1961) 652 pp.